Simulation of a Novel Phase Retrieval Technique for Multi-axis Robotic Arm Based Near-Field Antenna Measurements

C.G. Parini[1], S.F. Gregson[1, 2]
[1] Queen Mary University London, London, UK, c.g.parini@qmul.ac.uk
[2] Next Phase Measurements LLC, CA, USA, stuart.gregson@qmul.ac.uk

Abstract— **The simulation of a novel robot-arm based near-field/far-field (NF/FF) antenna measurement system enabling the reconstruction of measured AUT phase without the need for a phase reference cable is described. The mathematical approach follows the principle used within GPS position and time recovery. This work addresses the need for industrial robot arm-based NF/FF antenna measurements at both microwave and importantly millimetrewave frequencies where the transmitting probe RF phase reference cannot be guaranteed to be provided with the necessary stability by cable management or rotary joints. To assess the viability a computer simulation of the measurement system is constructed, and its performance analysed in terms of the accuracy of reconstruction of the AUT phase and true NF probe location, as well as the NF/FF radiation pattern accuracy in terms of Equivalent Multipath Level (EMPL). We demonstrate that a microwave system can offer EMPL below -60dB and that a millimetrewave system operating from 40GHz to 100GHz can offer EMPL below -50dB.**

Index Terms—near-field to far-field, antenna measurements, robot arm positioners, phase retrival.

I. Introduction

Antenna measurement systems incorporating multi-axis robotic positioners, are generally capable of acquiring spherical, cylindrical and variable orientation planar near-field data as well as taking far-field and extrapolated gain measurements; with the flexibility of the system meaning the user is not limited to purely these choices [1]. The extreme adaptability of the system affords the test engineer unique opportunities to acquire highly accurate, uniquely tailored measurements, that are not available from other more traditional antenna test systems. Industrial robots also offer a cost-effective solution compared to custom designed positioning systems. However, unlike the custom designed systems, there is seldom the opportunity to insert rotary RF joints in each of the robot axes (6 in this case) and so RF cable management becomes an increasing significant issue as the frequency of operation rises. As is known [2] the ultimate limit to the accuracy in a Near-Field (NF) measurement system is dominated by both the positional and phase accuracy. For Near-Field to Far-Field (NF/FF) antenna measurements the need to measure both amplitude and phase at each point in NF scan means that highly phase stable coaxial cable must be employed and managed from the base of the robot to the probe antenna mounted at the robot arm head, which typically crosses 6-axes. Whilst this is achievable (with difficulty!) using commercial cable management systems at microwave frequencies, it becomes a major problem when moving to millimetrewave operation. A possible solution to this problem is to use a self-contained millimetrewave source and probe antenna mounted at the robot arm head and employ phase retrieval to determine the phase of the transmitting probe. Conventional phase retrieval techniques offer many problems with inconsistent results [3]. Recently the authors have proposed a novel phase retrieval system [4] for use in drone-based NF/FF measurements at microwave frequencies which is based on the use of multiple reference antennas surrounding the antenna under test (AUT). The mathematical approach of the method follows the principle used within Global Positioning Systems (GPS) position and time recovery. Conceptually the satellites are replaced by ground-based reference antennas of known location, the user location is now the drone location and the user clock offset is replaced by the unknown AUT phase radiation at the angle subtended between the AUT and drone location. For the system to work the approximate location of the drone probe needs to be determined to within a wavelength of the actual location, which using differential GPS limits the system to use up to about 12GHz.

In this paper we develop the approach of [4] for the case where the NF probe is mounted on a robot arm and the location of the probe is known to a high degree of accuracy, for example 0.1mm. With this level of positional accuracy, we show that the system can offer good performance up to 100GHz.

II. The Near-Field Phase Retrieval Process

As described in the introduction, the proposed measurement system is based around the mathematical principals of GPS. Here the VNA (Vector Network Analyser) measured phase difference between one of four (or more) reference antennas (REF) and the AUT when the system is illuminated by the transmitting robot arm-based probe provide four (or more) equations in the four unknowns of the AUT phase and the unknown coordinates of the probe, enabling these unknowns to be solved. Such VNAs are commercial off the shelf products (COTS) and are available

from several suppliers [5]. Based on the work of [4] a system using 6 reference antennas was found to be optimal and has been employed in this work. A diagram showing the proposed measurement system for millimetrewave operation is shown in Fig. 1.

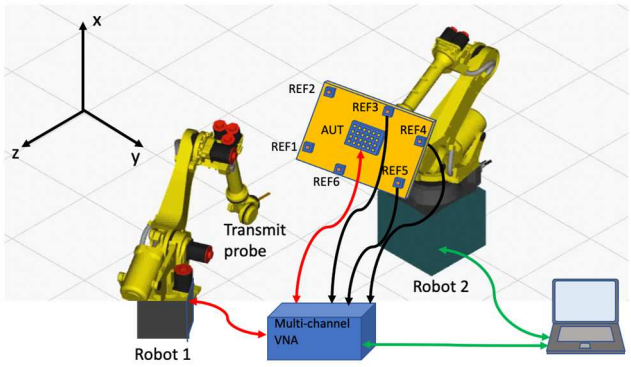

Fig. 1. Robotic arm measurement concept showing the millimetrewave configuration with 6 REF antennas (just three of the 6 REF antenna connections to the VNA are shown for clarity)

Here, the multichannel VNA enables the phase difference between the signal received from the probe by the AUT and the signal received from the probe by each REF antenna to be measured simultaneously with a trigger from the control system. The true location of the probe is P at coordinates (t_x, t_y, t_z) and this we aim to determine along with the unknown AUT phase, ϕ_{AUT}. The system also records the location of the probe P' at coordinates (d_x, d_y, d_z) via the robotic arm control system, which as mentioned above can have a repeatability accuracy of 0.1mm.

Full details of the mathematical approach of the phase reconstruction can be found in [4] and so just the basic mathematics will be presented here to aid the readers understanding. Fig. 2 shows a possible test set up, with the robot arm mounted probe at its true location, P. Then, the pathlength difference expressed as a phase difference, ϕ'_{Rn}, between the signal from the probe at P to the AUT at coordinates (a_x, a_y, a_z), and the probe to the n^{th} REF antenna, R_n, at coordinates (r^n_x, r^n_y, r^n_z), is given by:

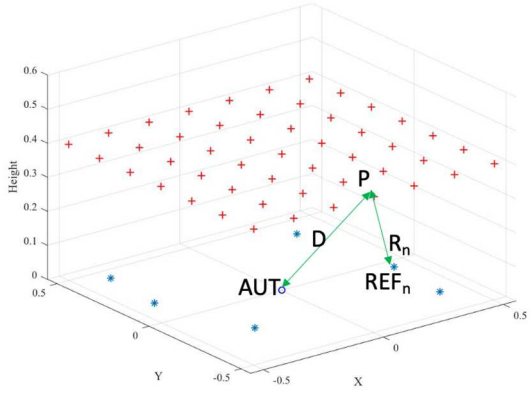

Fig. 2. Measurement set-up: AUT (blue circle) surrounded by 6 REF antennas (blue stars), 49 NF probe measurement points (red crosses); Example of path lengths D and R1 are also shown. Dimensions in metres.

$$\phi'_{Rn} = k\,R_n - (k\,D - \phi_{AUT}) \quad (1)$$

where:

$$R_n = \sqrt{(t_x - r_x^n)^2 + (t_y - r_y^n)^2 + (t_z - r_z^n)^2}$$

and:

$$D = \sqrt{(t_x - a_x)^2 + (t_y - a_y)^2 + (t_z - a_z)^2}$$

with k the free-space wavenumber and using a positive $(+j\omega t)$ time-convention assumed.

The path difference expressed as a phase, ϕ'_{Rn}, consists of the measured phase, ϕ_{Rn}, and an unknown number of full wavelengths N_n, thus,

$$\phi'_{Rn} = \phi_{Rn} + 2\pi N_n \quad (2)$$

However, we have a strong estimation of N_n from knowledge of the robot arm location of the probe $P'(d_x, d_y, d_z)$, giving:

$$N_n = \mathbf{int}\left[k(R'_n - D')/2\pi\right] \quad (3)$$

where:

$$R'_n = \sqrt{(d_x - r_x^n)^2 + (d_y - r_y^n)^2 + (d_z - r_z^n)^2}$$

and:

$$D' = \sqrt{(d_x - a_x)^2 + (d_y - a_y)^2 + (d_z - a_z)^2}$$

If we choose a measurement frequency such that the probe position error is less than or equal to the wavelength, then the true value of N_n will be known to within ±1. Thus, for the case of four REF antennas, equation (1) forms a set of four simultaneous equations in the four unknowns of the true location of the probe $P(t_x, t_y, t_z)$ and the AUT phase, ϕ_{AUT}. These equations can be solved using the Newton-Raphson method, or for the 6 REF antenna system used here, the method of Least Squares [6].

The above formulation assumes that:

i) We can accurately determine the physical locations of the phase centres of the REF antennas relative to a reference point, (a_x, a_y, a_z) on the AUT aperture. In practice, the REF antennas and AUT will have physical reference points marked on them and the phase centre is *a priori* known to that point. The Cartesian coordinates of the REF antennas relative to (a_x, a_y, a_z) can then be measured using the robotic arm with a contact measurement probe as used in metrology laboratories (see for example [7]).

ii) The location of the probe $P'(d_x, d_y, d_z)$ is determined relative to the probes phase centre. In practice the location of the robot arm will be made relative to a datum on the robot arm and so a translation to the probe antenna phase centre needs to be made. The reconstructed true probe location $P(t_x, t_y, t_z)$ is thus made relative to the probe transmit antenna phase centre.

iii) The probe transmit antenna is typically a single polarised low gain probe. We assume that the probe transmit antenna pattern would have a low gain radiation pattern in the forward hemisphere to keep physical size and weight small, and to ensure a sufficiently strong signal illuminates all the REF antennas at every location of the probe as it transverses the synthesised NF measurement surface. Ideally NF/FF transformation requires both hands of polarisation to

be measured at the SAME point and the head rotation axis of the robotic arm provides this function. The probe antenna should ideally exhibit a flat phase function of the type typically used as GPS antennas. However, correction for the probe antenna phase pattern as a function of radiation angle is possible within the formulation

iv) As with the probe, the REF antenna should ideally exhibit a flat phase function of the type typically used as GPS antennas and again correction for the REF antenna phase pattern as a function of radiation angle is possible within the formulation.

v) The NF measurement scanning is fully undertaken by Robot 1 in fig.1 and Robot 2 merely provides the function of holding the AUT and REF antenna platform in a fixed position and could be replaced by a rigid platform. It is shown here as the proposed system forms part of a more general purpose antenna test facility employing multiple robot arms, as for example in [1].

III. A MATLAB SIMULATION OF THE MEASUREMENT SYSTEM

In order to evaluate the viability of the proposed measurement system a simulation of the measurement process was constructed in Matlab and follows that described in [4]. The basic experimental system is depicted in Fig. 2, which shows the case where the AUT is surrounded by six reference antennas (blue stars). The probe transmits the microwave test signal at each of the 49 designated NF measurement points (red crosses), of which one, at point P, is shown in the figure. From point P the transmitted signal is received by the AUT and all the REF antennas, and the multiport Vector Network Analyser (Fig.1) simultaneously measures the phase difference between the AUT (connected to the VNA reference port) and each of the REF antennas, hence measuring the path difference $D - R_n$ (for the n^{th} REF antenna) as a phase, ϕ_{Rn}. The accuracy to which this phase can be measured will be a factor in the system performance and as a baseline we have taken this accuracy to be 2° RMS (the effect of this parameter was studied in [4]). To produce the errored phase value we use a uniformly distributed random number generator which yields a peak-to-peak variation in phase of ±3.5° for the 2° RMS setting. The accuracy to which we can place the probe at a desired measurement point is dependent on the accuracy of the robotic arm and as a starting point we have used 0.1mm. In the simulation we thus place the true position of the probe at the regular grid position, P, (red crosses of Fig. 2) but give its recorded probe position, P', as a random location within a box of dimension (0.1 x 0.1 x 0.1) mm centred at the desired probe location. The simulation then proceeds by determining the 6 'measured' phases by calculating the path difference $D' - R'_n$ and from the wavelength determining a phase. At each 'measurement' point, P', the set of 6 measured phase values are repeated 10 times to account for the phase measurement error. For the simulation each of the 60 phase measurements have the random 2° RMS noise added. Full details of the simulation process can be found in [4].

A. AUT Phase and Probe Position Reconstruction

We first study the effect of the reference antenna location on the AUT phase and probe location recovery process for a system operating at 40GHz. Just as in the case of satellite DGPS locations where the best user location accuracy is achieved with a well spread satellite constellation about the user, here a well distributed REF antenna location about the AUT and measurement plane offers the best reconstruction performance.

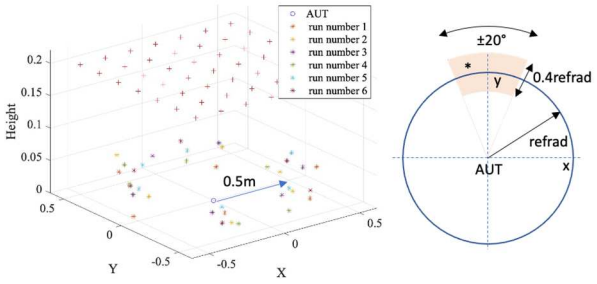

Fig. 3. Left: Six different runs for the 6 REF antenna locations placed around a nominal radius (refrad) of 0.5m. Right: Plan view diagram showing shaded area within which a REF antenna (*) is randomly placed for each run.

To this end, Fig. 3 (left) shows six different runs for the 6 REF antenna locations (labelled *) placed pseudo-randomly around a nominal radius (r_{ref}) of 0.5m. To the right of Fig.3 is a plan view diagram showing the shaded area within which a REF antenna (*) is randomly placed for each run. In addition, the height of each REF antenna relative to the AUT is randomly varied over a range 0 to 50mm.

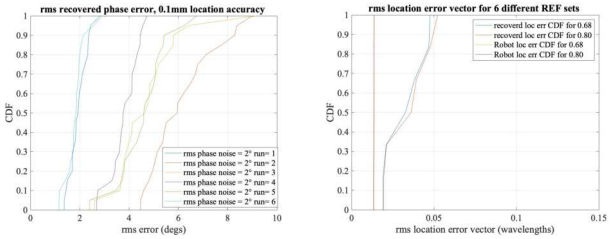

Fig. 4. Six REF antenna performance of the 6 different REF antenna location runs. Frequency = 40GHz, RMS phase measurement error =2°. (a) CDF of recovered rms phase error over each of the 49 NF sample points. (b) CDF of recovered rms probe location error vector with the results of each run shown in (a) plotted at both the 68% CDF and 80% CDF points.

The results for each of these six sets of REF antenna location runs is shown in Fig. 4(a), where each REF antenna set is run 20 times and from these results a Cumulative Distribution Function (CDF) for the recovered phase RMS error over the 49 sample points is determined. Runs 1 and 6 offer the lowest recovered phase error, with run 2 being worst by a factor of about three. Clearly use of the simulation to choose an optimal location for the REF antennas is valuable. Fig. 4(b) shows the corresponding CDF of recovered RMS probe location error vector magnitude (at CDF of 68% and 80%) over the 6 runs of REF antenna

locations. Also shown is the CDF of the probe RMS error location vector based purely on the statistics of the robot arm location accuracy of 0.1mm. In this case we see that because of the high precision offered by the robot arm there is no need to use the recovered probe position as this is less reliable than the position which is provided by the robot arm control system. This is contrary to the conclusion found in [4] for the case of a drone positioned probe where the drone position error is only poorly known because of the use of DGPS. We have found from the simulations that if the robot arm positioning error (of both the probe and along with the positions of the REF antennas during the initial calibration process) exceeds about 0.07λ then it becomes necessary to use the recovered probe positions as these give a more accurate location for the NF measurement point. For 40GHz this switch point would be at a position error value of about 0.5mm.

B. Near-Field to Far-Field Antenna Measurement Performance

In this section we model the complete planar NF/FF measurement process, and Fig. 5(a) shows the system used for 40GHz operation using the single beam-formed RF output from a linearly polarised (in x) 28 x 20 element array antenna (elemental dipoles with 0.5λ element spacing) as the AUT.

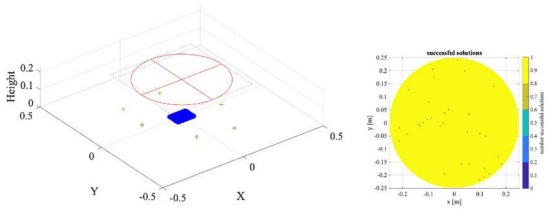

Fig. 5. (a) NF measurement of 28 x 20 array antenna at 40GHz probe height = 210mm, scan radius = 0.25m, sample spacing over cap = 0.425 wavelengths . (b) Sample locations where phase recovery failed giving error rate of 0.22%.

In this case we have taken a probe zenith height of 210mm, along with a 250mm scan radius. As in [4] we make allowances for the failure rate by using a NF sample spacing of 0.425λ. Fig. 5(b) shows a plan view of the scan plane with the sample locations where phase recovery failed shown as blue dots.

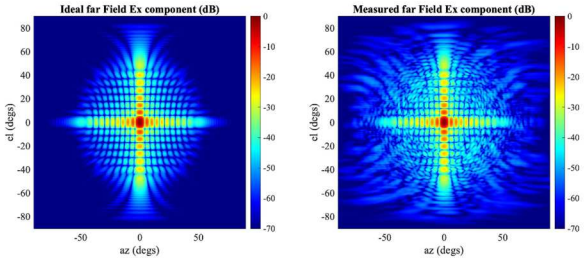

Fig. 6. Far-field co-polar pattern of array antenna of Fig. 5 at 40GHz. (left) True pattern. (right) Pattern 'measured' by robot with a rms phase measurement error of 2°

At these failed sample points we use a complex field interpolation scheme based around the four surrounding sample points to obtain an estimate of the complex field at the location of the failed sample point. Fig. 6 compares the FF co-polar pattern of the AUT obtained using the exact NF values (using for example a Plane Wave Spectrum NF/FF transform for non-uniform sample points [5]) with no measurement error (left) to that obtained with the AUT phase recovery process described in this paper (right hand figure). The phase radiated by the probe at each REF antenna needs to be adjusted for radiated phase pattern of the probe antenna, and this is simply achieved within the reconstruction software as the geometry of the complete probe REF antenna system is fully known. The reconstruction failure rate, using a VNA RMS phase measurement error of 2°, over the 25,281 measurements was 0.2%; the RMS recovered phase error was 2.7° (with a maximum of 14.6°).

To quantify the level of FF pattern error, Fig. 7 shows the Equivalent Multipath Level (EMPL) [2] for an azimuth radiation pattern cut. The full hemispherical FF pattern has an RMS EMPL level of -59.4dB and this is compatible with what can be achieved in conventional NF/FF facilities.

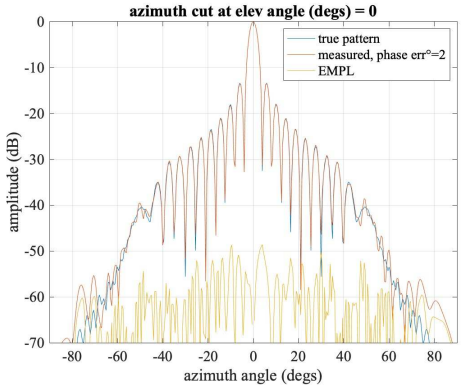

Fig. 7. Left: Azimuth cut of radiation pattern of 28 x 20 element array 'measured' at 40 GHz over a scan radius 0.25m, robotic arm height 210mm, nominal REF antenna radius = 0.25m, Ref antenna position accuracy 0.1mm (0.013l), rms phase measurement error = 2°.

C. Operating Parameters

In this section we first look at the operating parameters for millimetrewave operation. The first 3 rows of Table 1 show the effect on the 40GHz transformed FF pattern EMPL of different values of robotic arm positioning repeatability from 0.5mm to 0.05mm. In the simulation this level of positional accuracy is applied to both the probe location during the probe scanning and the location of the REF antennas relative to the AUT which is performed during the initial calibration process. We note that Fanuc quotes repeatability for its 45M and 270F robotic arms (typically 2.6m reach) of ±0.6mm and ±0.5mm respectively so the use of 0.1mm peak-to-peak in this paper is highly realistic and thus offers very good performance with EMPL level of -59.4dB and low failure rate. The next two rows show that 60GHz performance is equally good with 0.1mm location

accuracy (EMPL of -56.3dB). The last three rows consider 100GHz performance and again with 0.1mm location accuracy a very acceptable EMPL level of -51.6dB is achieved. Also shown in the 100GHz results is the effect of a 0.2mm and 0.05mm position accuracy. For the 100GHz case the 28 x 20 array is physically much smaller than the 40GHz antenna, so we have reduced the nominal radius of the location of the REF antennas (Refrad) as well as the size of the NF scan radius and probe to AUT height to limit the number of NF points needed.

TABLE 1: MILLIMETREWAVE SYSTEM NF/FF EMPL PERFORMANCE FOR VARIOUS ROBOT POSITION LOCATION ACCURACIES

Frequency (GHz)	Refrad /scan radius (m)	robot location error (mm)	probe to AUT distance (mm)	EMPL (dB)	fail %
40.0	0.25	0.50	210	-45.2	7.5
40.0	0.25	0.10	210	-59.4	0.2
40.0	0.25	0.05	210	-63.4	0.4
60.0	0.25	0.10	210	-56.3	0.2
60.0	0.25	0.05	210	-61.1	0.3
100.0	0.13	0.20	100	-45.1	7.7
100.0	0.13	0.10	100	-51.6	0.2
100.0	0.13	0.05	100	-57.3	0.2

We next consider the use of the system at microwave frequencies, Fig.8, and as for the millimetrewave case the robot arm provides the location of the REF antennas relative to the AUT during an initial calibration phase as well as the scanning of the NF probe. Table 2 shows the simulated results for Fig.8 at microwave frequencies again showing excellent FF EMPL levels below -60dB.

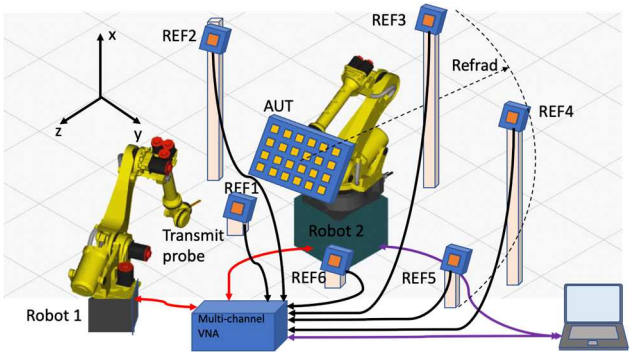

Fig. 8. Robotic arm microwave measurement concept. The nominal REF antenna location radius Refrad is shown on the right.

TABLE 2: MICROWAVE SYSTEM NF/FF EMPL PERFORMANCE FOR SEVERAL FREQUENCIES.

Frequency (GHz)	Refrad /scan radius (m)	robot location error (mm)	probe to AUT distance (mm)	EMPL (dB)	fail %
5.0	1.00	0.10	300	-61.4	0.3
10.0	0.50	0.10	300	-64.4	0.1
20.0	0.25	0.10	210	-63.8	0.4

IV. CONCLUSIONS

This paper has shown that standard industrial robotic arms can be effectively used in planar NF measurements at both microwave and millimetrewave frequencies without the need for the difficultly of managing the RF phase reference cable normally associated with NF measurements. The approach employs the use of six fixed reference antennas to reconstruct the true phase response of the AUT at a given probe location and is based on the same mathematical principles that are employed in satellite-based GPS. This process of phase recovery via reference antennas has the added bonus that long term phase drift, often a NF acquisition problem, is removed without the need for return-to-point calibration schemes, *etc*. The removal of the need for difficult (or very challenging at >40GHz) cable management or custom-built robotic arms with multiple RF rotary joints admits the use of standard industrial robots offering lower cost and multi-use antenna test systems within a single test chamber. Although we have here concentrated on the application of planar NF, the approach can be applied to non-canonical surfaces such a spherical cap that can offer improved far out sidelobe accuracy for a given NF scan radius.

V. REFERENCES

[1] D. M. Lewis, J. Bommer, G. E. Hindman and S. F. Gregson, "Traditional to Modern Antenna Test Environments: The Impact of Robotics And Computational Electromagnetic Simulation on Modern Antenna Measurements," *2021 15th European Conference on Antennas and Propagation (EuCAP)*, 2021, pp. 1-5, doi: 10.23919/EuCAP51087.2021.9411068.

[2] C. G. Parini, S. F. Gregson, J. McCormick, D. Janse van Rensburg, Thomas Eibert, "Theory and Practice of Modern Antenna Range Measurements, Second edition ", Vols. 1 and 2, IET Press, 2021, ISBN 978-1-83953-126-2.

[3] A. Paulus, J. Knapp, J. Kornprobst and T. F. Eibert, "Reliable Linearized Phase Retrieval for Near-Field Antenna Measurements With Truncated Measurement Surfaces," in *IEEE Transactions on Antennas and Propagation*, vol. 70, no. 8, pp. 7362-7367, Aug. 2022, doi: 10.1109/TAP.2022.3145383.

[4] Parini, C.G., et al, "Untethered near-field drone-based antenna measurement system for microwave frequencies using multiple reference antennas for phase and drone location recovery". IET Microw. Antennas Propag. (2022). https://doi.org/10.1049/mia2.12295

[5] "ZNBT Vector Network Analyzer: Specifications", Rohde & Schwarz, April 2020.

[6] Jacquelyne Ta, "Global Positioning System", A Thesis Presented to The Faculty of the Mathematics Program California State University Channel Islands, Degree Masters of Science, April, 2011.

[7] Zhiguang Jiang et al, "Automatic high-precision measurement technology of special-shaped surface parts based on robot arms", 2020 J. Phys.: Conf. Ser. 1693 012214.